J Polym Environ (2013) 21:151–159
DOI 10.1007/s10924-012-0480-z

ORIGINAL PAPER

Poly(Ethylene Glycol) as a Compatibilizer for Poly(Lactic Acid)/ Thermoplastic Starch Blends

Márcia Maria Favaro Ferrarezi · Márcia de Oliveira Taipina · Laura Caetano Escobar da Silva · Maria do Carmo Gonçalves

Published online: 29 May 2012

Abstract A new route to prepare poly(lactic acid) (PLA)/ thermoplastic starch (TPS) blends is described in this work using poly(ethylene glycol) (PEG), a non-toxic polymer, as a compatibilizer. The influence of PEG on the morphology and properties of PLA/TPS blends was studied. The blends were processed using a twin-screw micro-compounder and a micro-injector. The morphologies were analyzed by scanning and transmission electron microscopies and the material properties were evaluated by dynamic-mechanical, differential scanning calorimetry, thermogravimetric analysis and mechanical tests. PLA/TPS blends presented large TPS phase size distribution and low adhesion between phases which was responsible for the lower elastic modulus of this blend when compared to pure PLA. The addition of PEG resulted in the increase of PLA crystallization, due to its plasticizing effect, and improvement of the interfacial interaction between TPS and PLA matrix. Results show that incorporation of PEG increased the impact strength of the ternary blend and that the elastic modulus remained similar to the PLA/TPS blend.

Keywords Poly(lactic acid) · Thermoplastic starch · Poly(ethylene glycol) · Blend · Morphology

Introduction

Poly(lactic acid) (PLA) stands out among several biopolymers as it is a high modulus thermoplastic, can be derived from 100 % renewable resources and can be easily processed by conventional techniques [1–4]. If PLA is submitted to environmental conditions, it can degrade into carbon dioxide, methane and water over a period of months to 2 years. Its degradation is dependent on time, temperature, low-molecular weight impurities and catalyst concentration. On the other hand, PLA is very brittle under tensile and bending loads, presents low gas barrier and it is still an expensive material compared to the common synthetic industrial polymers, despite the new low-cost continuous process developed by Cargill Dow LLC [1–4].

Depending on the application, some polymer characteristics are essential and so then PLA properties should be improved. For example, the polymer for film technology must display high elongation and flexibility at room temperature. On the other hand, for disposable packages used in food industry, cheap resins with high biodegradation rate and moderate mechanical properties are required. These different characteristics can be achieved by adding biocompatible plasticizers to PLA [5–7], by mixing PLA with other polymers [8–14] or by incorporating specific fillers [15–17].

Interesting biodegradable polymer candidates to be blended with PLA are polysaccharides, such as starch and cellulose, due to their abundant availability, compostability and non-toxicity. Particularly thermoplastics composed of starch are one of the cheapest functional "green" materials. However, the native starch has to be modified in order to be melt processed as a thermoplastic, since its melting temperature is in the range of 220–240 °C and its onset degradation temperature is around 220 °C [7, 10, 18, 19]. In this case, the starch granular structure should be disrupted by using plasticizers, mainly water and/or glycerol, under heating and shear procedures, resulting in a viscous melt continuous phase, denoted as thermoplastic starch (TPS)

M. M. F. Ferrarezi · M. de Oliveira Taipina · L. C. Escobar da Silva · M. C. Gonçalves (✉)
Institute of Chemistry, University of Campinas (UNICAMP), P. O. Box 6154, Campinas, SP, Brazil
e-mail: maria@iqm.unicamp.br

[1, 19, 20]. Some authors [7, 21] recognized that water is a more efficient plasticizer for starch; on the other hand, the majority of the engineering plastics that can be blended with starch can be depolymerized in the presence of water at elevated temperatures, which results in the decrease of mechanical properties [7].

Several papers in PLA/TPS blends have been reported [7, 10, 17, 22]. Martin and Avérous [22] melt blended PLA with thermoplastic starch and showed a low level of compatibility for this immiscible blend. Similar results were obtained by Park et al. [10]. These results were expected, as aliphatic polyesters (such as PLA) are hydrophobic, whereas starch is a hydrophilic material. Thus, this lack of affinity between PLA and starch is responsible for the formation of blends with poor mechanical properties.

On the other hand, some studies [6, 7, 9, 12, 23] describe grafting and/or incorporation of reactive groups in PLA or TPS chains to allow the compatibilization between the phases. Ren et al. [12] studied the effect of a compatibilizer with anhydride functional groups on the interfacial stability between PLA and TPS phases. The addition of the compatibilizer improved the interfacial adhesion, due to reactions between anhydride groups from the compatibilizer and hydroxyl groups from the TPS, generating ester links. The compatibilized blend showed an increase of flexural strength and flexural modulus compared to the properties of the non-compatibilized PLA/TPS blend. Huneault and Li [9] successfully obtained compatibilized PLA/TPS blends using a compatibilizer with maleic anhydride groups. The blends showed improved ductility and elongation at break. Recently, Ning et al. [6] studied the influence of citric acid as an additive, as it increases the fluidity of TPS, for the PLA/TPS blend. Infrared spectroscopy results showed that the citric acid generated interactions between PLA and TPS. Also, an increase of elongation at break was observed, but the tensile strength was negatively affected in almost all the studied conditions. Another reported study focusing on the improvement of the interfacial stability in starch blends was proposed by Carvalho et al. [23]. The authors treated starch surface with different agents, such as, isocyanates, styrene-co-glycidyl methacrylate and stearoyl chloride, which showed to be efficient in decreasing the starch hydrophilic character. The authors suggested that a degree of compatibility between the modified starch and biopolymers, such as PLA, could occur. In spite of some material property improvement that was obtained in some of these works, the use of compatibilizers has to take into account their composition since they can bring some degree of toxicity to the blends.

In this work, a simple route to prepare PLA/TPS blends is proposed using poly(ethylene glycol) (PEG), a non-toxic polymer, as a compatibilizer. Several reported works show that PLA/PEG blends present miscible to partially miscible behaviors, depending on the blend composition and polymer molecular weights [24–28]. Moreover, below 30 %wt of PEG content, PEG can act as a plasticizer for PLA, yielding higher elongations [24]. On the other hand, some reported works [29, 30] indicate that poly(ethylene oxide) (PEO) and PEG are miscible or partially miscible with starch, due to hydrogen bond interactions between the components. Based on these findings, it is expected that PEG can act as an adequate compatibilizer for PLA/TPS blends, by promoting favorable interfacial interactions between the components. So, the use of PEG as a third component in the PLA/TPS blends can result in the control of the phase morphology and in the improvement of the mechanical properties of these blends.

Experimental

Materials

Poly(lactic acid) (PLA), with a weight-average molecular weight (M_W) of 300,000 g/mol, was supplied by Nature Works and cassava starch was supplied by Copagra (Paraná, Brazil). Glycerol was obtained from LabSynth. A poly(ethylene glycol) (PEG), with M_W of 4,000 g/mol, was obtained from Aldrich. PEG molecular weight was chosen for this study based on the work developed by Kim et al. [30], which showed that starch chain conformation changed when starch and PEG chains, with molecular weight <8,000 g/mol, are mixed.

Processing of the Blends

To plasticize the starch, 40 %wt of glycerol was added to native dry starch, then mixed and allowed to sit overnight to facilitate the glycerol diffusion into the starch granules. This mixture was fed into a twin-screw DSM Xplore micro-compounder. The mixing speed was set at 50 rpm and the chamber temperature was 150 °C. The processed TPS was pelletized. Binary and ternary blends were also processed in the micro-compounder. PLA and TPS pellets were dried under vacuum at 70 °C for 6 h before processing. Table 1 shows the blend compositions. All the blends were processed at 180 °C and 100 rpm for 1 min. A residence time of 1 min was chosen to minimize the PLA and TPS degradation during high shear rates.

Two methodologies were applied for the ternary blend preparation (one-step and two-step mixing procedures). In the blends processed by the one-step procedure, all the three components (PLA, TPS and PEG) were mixed together in the extruder in only one step. In the other case, of the blends processed by the two-step mixing procedure

Table 1 Compositions of the processed blends

Samples	PLA (%wt)	TPS (%wt)	PEG (%wt)
PLA/TPS	75	25	–
PLA/PEG	75	–	25
TPS/PEG	–	75	25
PLA/TPS/PEG-1[a]	56	19	25
PLA/TPS/PEG-2[b]	56	19	25

[a] PLA/TPS/PEG-1 = ternary blend obtained by one-step mixing procedure

[b] PLA/TPS/PEG-2 = ternary blend obtained by two-step mixing procedure

PLA/PEG (75/25 %wt) and TPS/PEG (75/25 %wt) blends were firstly processed separately and then these blends were mixed to obtain the (56/19/25 %wt) PLA/TPS/PEG ternary blend.

The materials were injection molded in a DSM Xplore micro-injector in order to prepare typical tensile and impact specimens, according to ASTM-D256 and ASTM-D1708 standards. The mold and injection temperatures were 40 and 180 °C, respectively. The pressure and packing time profile during the injection process was 6 bar for 5 s and 8 bar for 10.7 s.

Characterization of the Materials

Samples, for all the morphological, thermal and dynamic-mechanical characterization were removed from the central region of the injected specimens. These samples were dried under vacuum at 70 °C for 6 h before characterization.

The morphologies of the samples were examined with a JSM-6340 field emission scanning electron microscope (FESEM) from Jeol Ltd., operating at an accelerating voltage of 3.0 kV. The samples were prepared by fracturing in liquid nitrogen followed by carbon and gold sputtered coating in a Bal-Tec MD 020 instrument (Balzers). The morphologies of the samples were also investigated in a Carl Zeiss CEM902 transmission electron microscope (TEM). The microscope was operated at an acceleration voltage of 80 kV and equipped with a Castaing-Henry energy filter spectrometer within the column. Ultrathin sections, approximately 65 nm thick, were cut at ~−100 °C using a diamond knife, in a Leica EM FC6 cryo-ultramicrotome. The images were recorded using a Proscan high-speed slow-scan CCD camera and processed using the Analysis software.

Dynamic-mechanical behavior of the blends was analyzed using a DMTA V Rheometric Scientific Instrument from −120 to 160 °C using a 2 °C/min heating rate, a fixed frequency of 1 Hz and amplitude of 0.02. Infrared spectra were performed on a Bomem MB B100 Series spectrometer operating at 4 cm^{-1} resolution and co-adding 16 scans over the 400–4,000 cm^{-1} range. Differential scanning calorimetry analysis (DSC) were conducted on a DSC model 2910, TA Instruments. The thermal curves were obtained from −90 to 200 °C at a 10 °C/min scanning rate and under an argon flow. Thermogravimetric analysis (TGA) was performed in a TA 2950 thermobalance, TA Instruments, over the 25–700 °C range, at a 20 °C/min scanning rate under an argon flow.

The injection molded specimens were submitted to impact resistance (Izod method) and tensile tests in an EMIC AIC 1 and in an EMIC DL 200 apparatus, following ASTM-D256 and ASTM-D1708, respectively. At least five measurements for each sample and test were done.

Results and Discussion

Figure 1 presents the morphologies of the cryogenic fracture surfaces of the samples investigated by FESEM. PLA presented a smooth surface, characteristic of a brittle semi-crystalline polymer (Fig. 1a). On the other hand, the fractured surface morphology of PLA/TPS blend in Fig. 1b was relatively rough, showing TPS dispersed phases and cavities generated due to TPS phase detachment during sample fracture. The absence of interactions between the phases is demonstrated by the low adhesion between PLA and TPS phases. A large distribution in TPS domain size was also observed. This characteristic morphology was also reported in literature [10, 22] and is attributed to the expected low affinity between the hydrophobic PLA and the hydrophilic TPS phases.

In the case of PLA/PEG and TPS/PEG blends (Fig. 1c, d, respectively) no evidence of phase separation was detected by this technique.

The ternary blend fractures in Fig. 1e, f showed large domains. Both ternary blends presented dispersed TPS domains and pores distributed in the PLA matrix. The reason for the formation of pores in the matrix is not clear. Possible explanations could be attributed to trapped air in the polymer or to water and other volatile compounds released during blend processing, which was carried out at 180 °C.

The TEM images have complemented the FESEM analysis, allowing a better observation of the blend phase interfaces. Figure 2 shows the TEM micrographs of PLA/TPS and PLA/TPS/PEG-2 blends. There was no need to stain the microtomed TEM samples as the phase contrast was good enough to identify the different phases, where the TPS phase is the bright phase and the PLA matrix is the dark phase. The PLA/TPS blend morphology (Fig. 2a) consisted of dispersed TPS domains in the PLA matrix; also, the interface between these TPS domains and PLA matrix was clearly defined. However, there is a significant difference on the interface aspect in the presence of PEG.

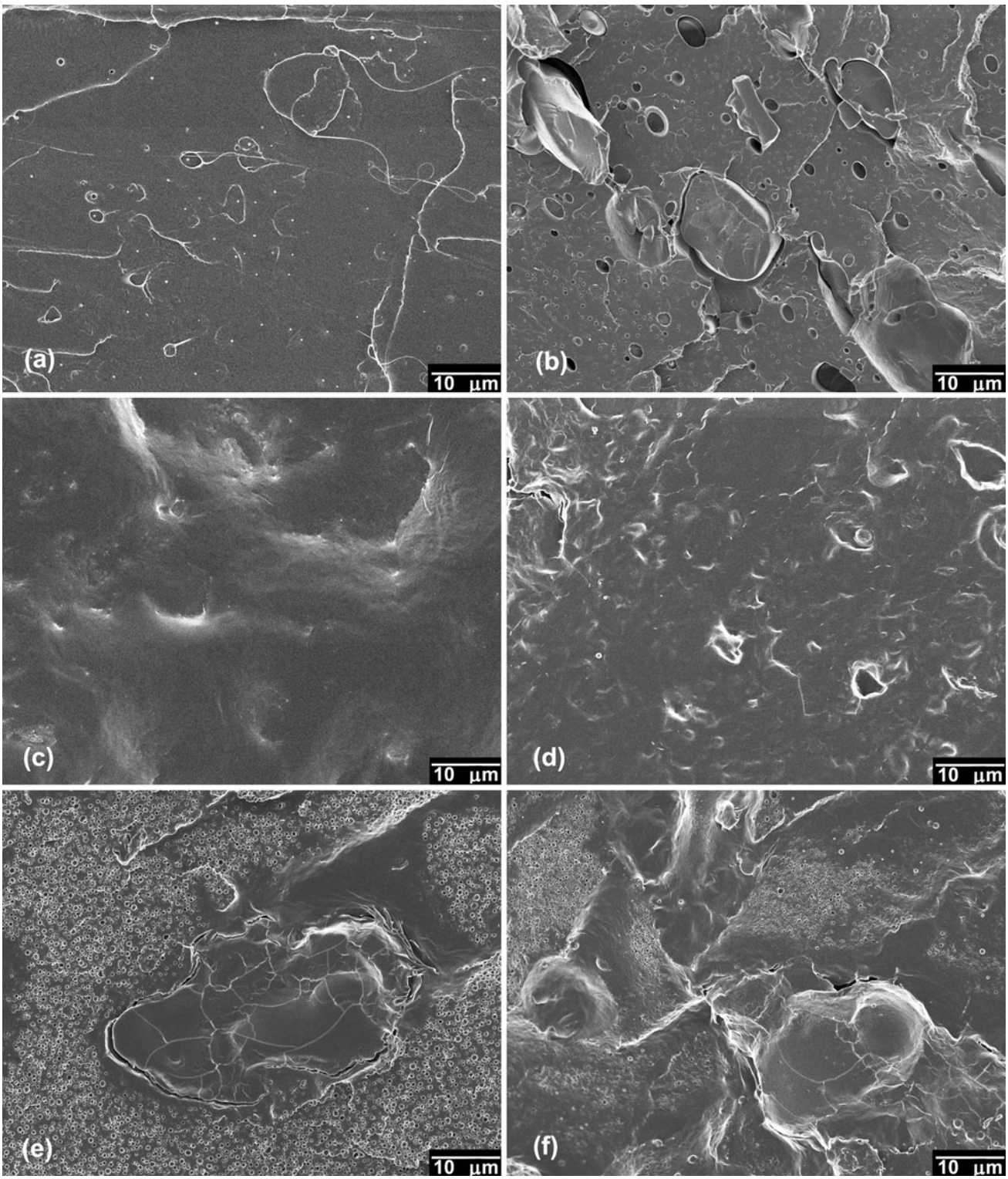

Fig. 1 FESEM micrographs of fracture surfaces: **a** pure PLA, **b** PLA/TPS, **c** PLA/PEG, **d** TPS/PEG, **e** PLA/TPS/PEG-1 and **f** PLA/TPS/PEG-2

When PEG is present in the ternary blend (Fig. 2b) the interface between the TPS and PLA phases is more diffused, indicating that PEG chains probably acted as a compatibilizer agent between PLA and TPS phases. This was responsible for the enhancement of the interface strength, which could be directly related to the improvement on the impact mechanical properties of the ternary blends.

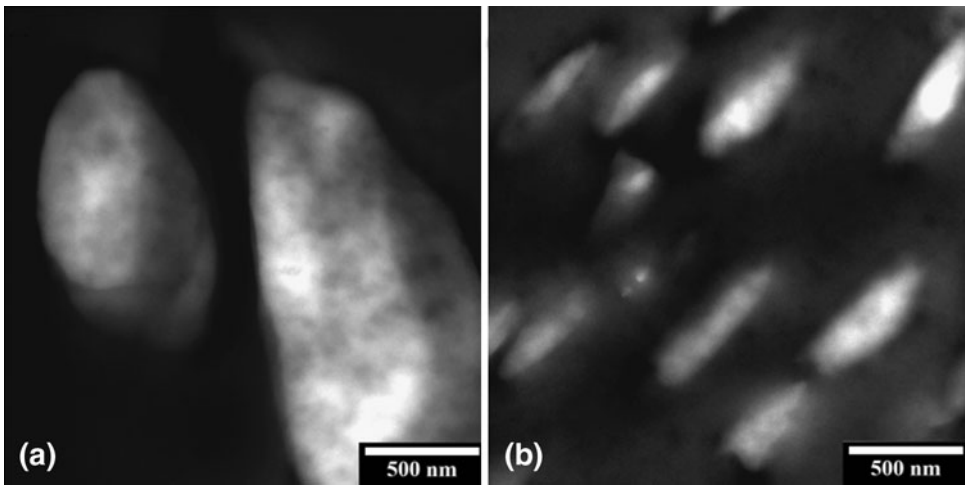

Fig. 2 TEM micrographs of: **a** PLA/TPS blend, **b** PLA/TPS/PEG-2 blend

Table 2 DMA and DSC results of pure polymers and blends

Samples	$T_{g(1)}$ (°C)[a]	$T_{g(2)}$ (°C)[b]	Peak width at ½ height of $T_{g(2)}$ (°C)[c]	T_{CC} (°C)[d] (PLA)	X_C (%)[e] (PLA)	X_C (%)[e] (PEG)
PLA	–	83	21	130	17.7	–
PLA/TPS	−57	71	14	107	41.1	–
PEG	–	–	–	–	–	85.7
PLA/PEG	−49	NM[f]	NM[f]	80	42.9	0.0
TPS/PEG	−62	–	–	–	–	43.2
PLA/TPS/PEG-1	−77/−48	67	37	81	49.6	27.2
PLA/TPS/PEG-2	−65/−46	40	30	84	46.8	42.0

[a] $T_{g(1)}$ = glass transition temperature related to the glass transition of TPS or PEG phase, obtained from the loss modulus curve

[b] $T_{g(2)}$ = glass transition temperature related to the glass transition of PLA phase, obtained from the loss modulus curve

[c] Peak width measured at the half height of the glass transition peak obtained from the tan(δ) curve

[d] T_{CC} = cold crystallization temperature, obtained during the second heating cycle

[e] X_C = crystallinity degree; for calculation of X_C of PLA and PEG, the following values of heat of fusion for 100 % crystalline polymer ($\Delta H°$) were used: $\Delta H°$ (PLA) = 93.7 J/g [38] and $\Delta H°$ (PEG) = 214.6 J/g [39]

[f] NM = not measured, as explained in the manuscript

Figure 3 and Table 2 show the main parameters obtained from the dynamic-mechanical analysis of the materials. PLA presented an intense relaxation with a maximum temperature of 83 °C attributed to its glass transition temperature (T_g). Based on reported results, TPS usually shows two transitions, one related to the α relaxation of starch, which depends on the glycerol content in the starch, and another in the range of −54 and −63 °C, attributed to the glass transition of glycerol [31]. For instance, the T_g of the starch from TPS with 30 % glycerol is around 2 °C, whereas with 36 % glycerol, the T_g is equal to −8 °C [22, 32]. Also based on reported results, PEG presents a T_g in the range of −17 and −98 °C, which is dependent on its molar mass and crystallinity degree [33]. For instance, the T_g of 4,000 g/mol PEG, obtained from DSC, is −61 °C [34], whereas the T_g of 6,000 g/mol PEG with high crystallinity degree is −17 °C [35].

The blends presented two glass transition temperatures: a lower temperature named $T_{g(1)}$ related to the glass transition either of TPS or PEG components, or both together in the case of ternary blends, and a higher temperature named $T_{g(2)}$ related to the PLA glass transition. The detection of two distinct T_g values indicates the presence of two phases in all blends, except for the TPS/PEG blend, which showed a miscible blend behavior. Only the $T_{g(1)}$ was able to be measured for the PLA/PEG blend. This result can be explained by two hypotheses: indication of a partial miscibility between the PLA/PEG blend components or overlapping of the PEG melting process with PLA glass transition temperature.

A decrease of $T_{g(2)}$ of the PLA/TPS blend when compared with the $T_{g(2)}$ of pure PLA can be observed in Table 2. This behavior can be attributed to the plasticization of PLA by the glycerol molecules, as also shown in

literature [10]. Even lower $T_{g(2)}$ values were obtained for the ternary blends, which can be attributed to plasticizing effects of glycerol and also of PEG. Moreover, comparing the ternary blends, a lower $T_{g(2)}$ value was observed for the PLA/TPS/PEG-2 than for the PLA/TPS/PEG-1 blend, which is an indication that the two-step mixing procedure was more effective to distribute the PEG chains in the blend phases. Supposing that PEG is acting as a compatibilizer at the interface, it is expected that the two-step mixing procedure resulted in a ternary blend with a more uniform PEG distribution in both PLA and TPS phases during the processing, as firstly PLA was allowed to interact with PEG and, TPS with PEG in a separate step. Also, a partial miscibility between the components in PLA/TPS/PEG-2 blend can be inferred, as a significant reduction of the $T_{g(2)}$ was observed. However, two transition peaks in the range of $T_{g(1)}$ value were observed in the ternary blends, showing that the separation between TPS and PEG chains also occurred.

Figure 3a shows the temperature dependence on the storage modulus (E′) for the materials. Sharp drops are observed around the glass transition temperature associated to the PLA phase, and slight changes are observed in the TPS glass transition region. This behavior confirms that the blend morphologies analyzed by FESEM can be described as dispersed TPS domains in a PLA glassy matrix. Also, it was observed in Fig. 3a that the blends were less brittle than pure PLA at the usual service temperature. For example, in the case of the PLA/TPS/PEG-2 blend a 50 % reduction of the E′ value, at 25 °C, was observed.

Furthermore, PEG addition also generated broader transition peaks (the peak width increased, as indicated in Table 2 and Fig. 3b). This behavior describes materials with a wide range of relaxation times [36]. The presence of PEG probably changes the microheterogeneity of the systems, i.e., PEG chains can cause the formation of a number of microenvironments with different compositions and different interaction densities in the blends. Typical interactions are hydrogen bonding between the hydroxyl groups from PLA or starch and hydroxyl, as well as oxygen, from the PEG units, which caused the broadening of the PLA glass transition peak. Another aspect to be considered is that esterification between PLA and PEG could also occur during processing.

Interactions between polymers could be followed with infrared (IR) spectroscopy. If two polymers present a specific interaction, such as hydrogen or dipolar interactions, changes in the spectra could be detected. It was observed from the IR spectra (Fig. 4) that the -OH band of the PLA/TPS blend shifted to high wavenumber (around 3,360 cm^{-1}) when compared to the spectrum of pure TPS (around 3,280 cm^{-1}). This shift can be an indication of glycerol migration from the TPS phase to the matrix.

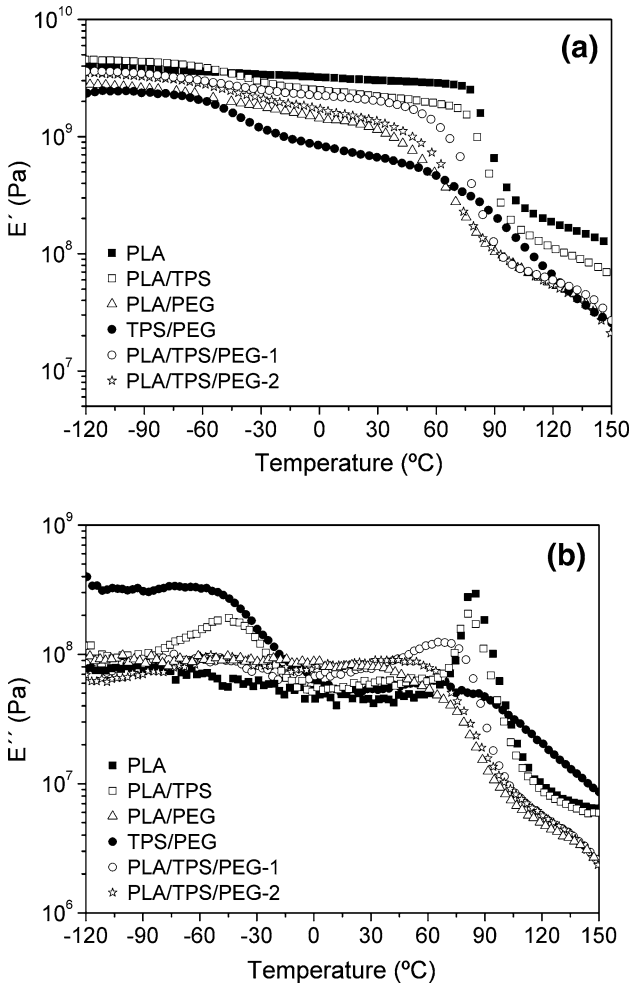

Fig. 3 Temperature dependence of **a** storage modulus (E′) and **b** loss modulus (E″) of pure PLA and blends

The thermal characteristics of the blends were determined by DSC and TGA. DSC results are shown in Table 2 and Fig. 5. PLA presented a melting temperature at 154 °C, a crystallization process during the heating step, giving a cold crystallization temperature (T_{CC}) of 130 °C, and a crystallinity degree (X_C) of approximately 18 %. PLA/TPS blend presented a lower T_{CC} and a higher X_C than pure PLA. This thermal behavior could be caused by two factors: the plasticizing effect of glycerol, which had migrated to the matrix blend and consequently enhanced PLA chain mobility and/or the presence of TPS domains, which could act as nucleating agents, accelerating the PLA nucleation process. Also, PLA developed a double melting peak (144 and 152 °C) in the PLA/TPS blend, which could be due to lamellar rearrangement during PLA crystallization [28] or the development of different crystalline structures [37].

Two interesting behaviors were observed for the PLA/PEG blend: the increase in the crystallization of PLA

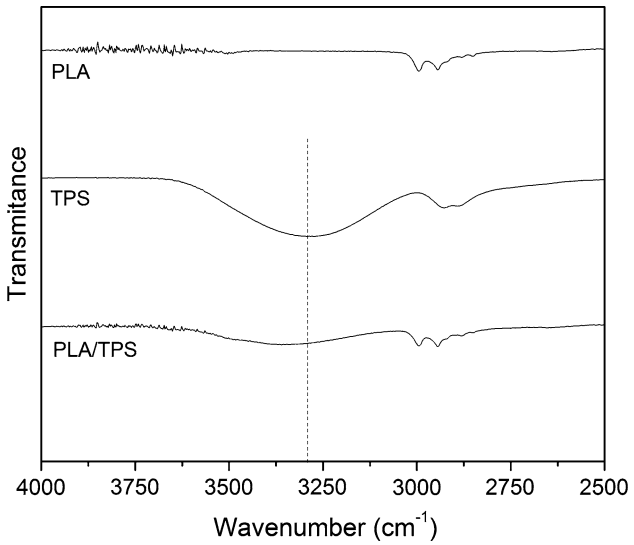

Fig. 4 FTIR spectra of pure PLA, TPS and PLA/TPS blend

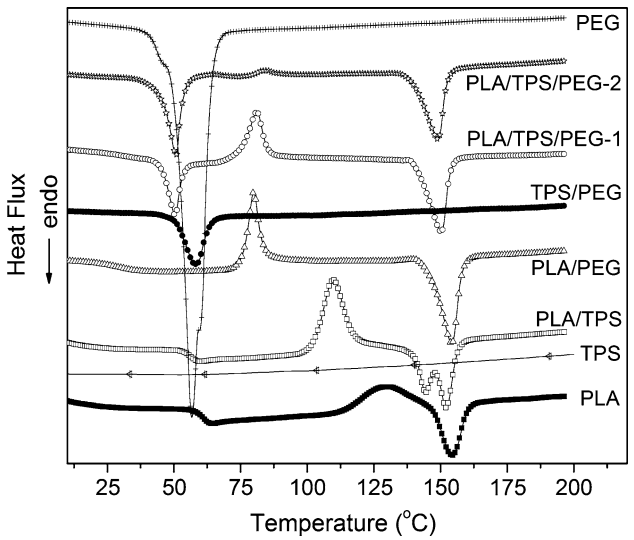

Fig. 5 Differential scanning calorimetry curves of pure polymers and blends obtained during the second heating

chains and the not detected crystallization of PEG chains. This result could be due to the high interaction developed between the components in the melt state. Supposing that the glass transition temperature of PLA phase in the PLA/PEG blend is higher than the crystallization temperature of PEG, PEG chains could be trapped inside the rigid matrix, which consequently could hinder crystallization and phase segregation. Sheth et al. [24] verified that the presence of PEG enhances PLA crystallization, as PEG acted as PLA plasticizer and consequently enhances the PLA chain mobility. However, as PEG chains could remain soluble in PLA, the PEG chains would not achieve their maximum crystallinity. This argument could also be applied in this

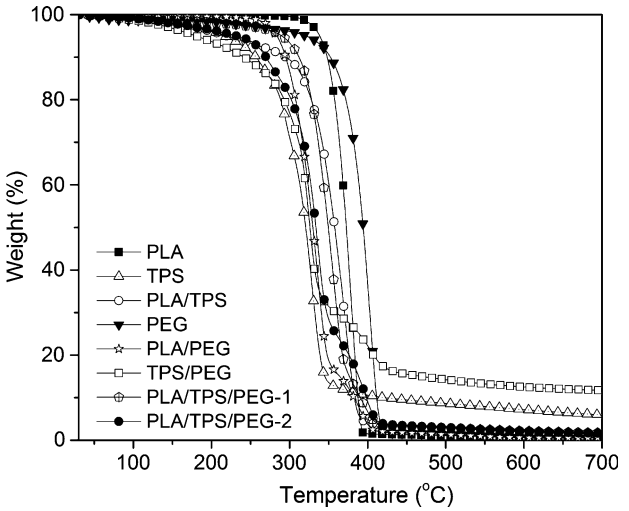

Fig. 6 Thermogravimetric curves of pure polymers and blends

work, as PEG crystallinity degree was significantly reduced in all blends (Table 2).

The changes in PLA crystallization process were even more significant in the ternary blends due also to the plasticizing effect of PEG. The T_{CC} values were reduced to approximately 40 % of the corresponding PLA value and X_C increases of around 260 % were obtained [38, 39]. Moreover, contrary to what happened in the PLA/PEG blend, PEG chains in the ternary blends crystallized. This behavior could be related to the PEG amount ratio in PLA. In the ternary blends the PEG content in relation to PLA was higher than the one in the PLA/PEG blend (as described in Table 1), thus, at this composition the PLA and PEG could not be miscible and phase separation could occur.

Also, the PEG crystallinity degree in the PLA/TPS/PEG-2 blend was significantly higher than that of the ternary blend obtained by one-step mixing (PLA/TPS/PEG-1). This difference can be explained analyzing the processing methodologies: during the preparation of PLA/TPS/PEG-1, PEG chains were distributed simultaneously in PLA and TPS phases, since both phases can interact with PEG. On the other hand, in the PLA/TPS/PEG-2 preparation, first PEG was mixed with PLA and separately with TPS. As the crystallinity degree of PEG in PLA/TPS/PEG-2 blend was the same as the one in the TPS/PEG blend, it is expected that a higher content of PEG was present in the TPS phase.

In relation to the thermogravimetry results (Fig. 6), PLA thermal degradation experiences a one-stage weight loss. The onset temperature (T_{onset}) of PLA thermal degradation was approximately 328 °C and the degradation was completed at about 395 °C. The PEG chain degradation started at 243 °C; the process occurred until 422 °C. On the other hand, thermoplastic starch presented a three-stage weight

loss. The onset temperature of TPS thermal degradation occurred at approximately 173 °C. The TPS degradation process was firstly related to water, volatile compounds and glycerol decomposition, followed by starch degradation [40, 41].

PLA/TPS, PLA/PEG and ternary blends presented intermediate thermal stability in relation to the pure polymers (T_{onset}(PLA/TPS) = 214 °C, T_{onset}(PLA/PEG) = 273 °C, T_{onset}(PLA/TPS/PEG-1) = 237 °C and T_{onset}(PLA/TPS/PEG-2) = 173 °C). The low T_{onset} of the PLA/TPS/PEG-2 can be due to matrix (PLA) degradation during the two-step processing method. Also, the residue content at 700 °C for PLA, PEG and the blends showed similar values (around 1 %), but for TPS the value was 7 %. These values are in agreement with the ones in literature [42].

On the other hand, TPS/PEG blend presented lower onset thermal degradation than the pure polymers (T_{onset}(TPS/PEG) = 135 °C), but the complete degradation temperature was similar to the pure polymers and a significant increase of the residue content at 700 °C (12 %) was observed, which could indicate that strong interactions occurred in this blend.

It is well known that the thermal decomposition of PLA is carried out by random chain or specific chain scissions because its repeated aliphatic ester structure is relatively easy to hydrolyze and break down. According to Mc Neill et al. [43] and Zeng et al. [44], the main reaction route is a non radical, backbiting ester interchange reaction involving –OH chain ends. Thus, the presence of the TPS phase may enhance the depolymerization of aliphatic ester in PLA, as the products of pyrolytic decomposition of starch include carbon monoxide, water, volatile organic compounds and a carbonaceous residue [39, 45].

Table 3 shows the mechanical properties of the studied materials. As expected, PLA presented high elastic modulus, high tensile strength at break, low elongation at break and low impact strength. With addition of TPS, the modulus and the tensile strength decreased but the elongation at break and the impact strength increased, due to the presence of the TPS ductile phase and also to glycerol migration to PLA. However, these increases were rather discrete due to the low compatibility between the phases in PLA/TPS blend.

Table 3 Mechanical properties of pure PLA and PLA blends

Sample	Impact strength (J/m)	Elastic modulus (MPa)	Maximum tensile strength (MPa)	Elongation at break (%)
PLA	22 ± 3	532 ± 43	71 ± 1	14 ± 1
PLA/TPS	55 ± 4	172 ± 34	41 ± 3	22 ± 2
PLA/PEG	43 ± 11	9.2 ± 0.8	23 ± 2	227 ± 29
PLA/TPS/PEG-1	119 ± 14	137 ± 17	16 ± 2	ND[a]
PLA/TPS/PEG-2	105 ± 4	121 ± 15	16 ± 1	ND[a]

[a] ND = value not detected by the equipment sensor

On the other hand, PLA/PEG blend showed a significant increase of the elongation at break (increase of approximately 1,650 % over the pure PLA values) and the impact strength of this blend was 200 % higher than that of pure PLA, confirming the PEG plasticizing effect. However, the elastic modulus decreased 98 % in relation to the one of pure PLA. To overcome this significant decrease in the modulus, studies of nanofiller addition, as cellulose whiskers and nanoclays, are being conducted in our research group and preliminary results will be published in a further article.

Lastly, the ternary blends showed a decrease in the tensile strength but an expressive increase of the impact strength (around 540 and 477 % higher than PLA for the one-step and two-step mixing procedures, respectively) when compared to pure PLA. However, comparing to the PLA/TPS blend, similar elastic modulus and higher impact strength were obtained for the ternary blends. It is well known that the phase size and interface strength of blend components are the key to determine the mechanical performance of a blend. Therefore, based on the results, it is possible to conclude that PEG chains acted as an efficient compatibilizer for the PLA/TPS blend, promoting chemical interactions between the phases and/or also acting as physical bridges. Strictly speaking, dispersed PEG chains in both PLA and TPS phases can develop entanglements that increase the strength at the blend interface.

Conclusions

Poly(lactic acid)/thermoplastic starch/poly(ethylene glycol) blends were prepared by melt extrusion and the efficiency of PEG as a compatibilizer was evaluated. In the absence of PEG, phase separation in PLA/TPS blends was observed through the presence of domains, with a low adhesion between the phases, which was responsible for the poor mechanical results when compared to pure PLA. PEG addition in the PLA/TPS blends probably caused the formation of a number of microenvironments with different compositions and interaction densities, which could be related to the increase of the interaction between the phase components; consequently the impact strength of the ternary blend (PLA/TPS/PEG) was significantly increased. It can be concluded that PEG chains acted as an efficient compatibilizer for the PLA/TPS blend by promoting

chemical interactions between the phases as well as acting as physical bridges.

Acknowledgments This research was supported by Conselho Nacional de Desenvolvimento Científico e Tecnológico (CNPq) and Fundação de Amparo à Pesquisa do Estado de São Paulo (FAPESP) (Brazil) through Inomat, National Institute (INCT) for Complex Functional Materials. The authors would also like to thank Cargill Dow and Copagra for material donation.

References

1. Yu L, Dean K, Li L (2006) Prog Polym Sci 31:576
2. Williams CK, Hillmyer MA (2008) Polym Rev 48:1
3. Gupta AP, Kumar V (2007) Eur Polym J 43:4053
4. Drumright RE, Gruber PR, Henton DE (2000) Adv Mater 12:1841
5. Li HB, Huneault MA (2007) Polymer 48:6855
6. Wang N, Zhang XX, Han N, Fang J, Thermopl J (2010) Comp Mat 23:19
7. Wang N, Yu J, Chang PR, Ma X (2008) Carbohydr Polym 71:109
8. Cai Q, Yang J, Bei J, Wang S (2002) Biomater 23:4483
9. Huneault MA, Li H (2007) Polymer 48:270
10. Park JW, Im SS (2000) Polym Eng Sci 40:2539
11. Shirahase T, Komatsu Y, Marubayashi H, Tominaga Y, Asai S, Sumita M (2007) Polym Degrad Stab 92:1626
12. Ren J, Fu H, Ren T, Yuan W (2009) Carbohydr Polym 77:576
13. Na Y-H, He Y, Shuai X, Kikkawa Y, Doi Y, Inoue Y (2002) Biomacromol 3:1179
14. Liao H-T, Wu C-H (2009) Mat Sci Eng A 515:207
15. Petersson L, Oksman K (2006) Comp Sci Technol 66:2187
16. Jacobsen S, Fritz HG (1996) Polym Eng Sci 36:2799
17. Arroyo OH, Huneault MA, Favis BD, Bureau MN (2010) Polym Compos 31:114
18. DeLeo C, Pinotti CA, Gonçalves MC, Velankar S (2011) J Polym Environ 19:689
19. Averous L, Halley PJ (2009) Biofpr 3:329
20. Smits ALM, Kruiskamp PH, Van Soest JJG, Vliegenthart JFG (2003) Carbohydr Polym 53:409
21. Hulleman SHD, Janssen FHP, Feil H (1998) Polymer 39:2043
22. Martin O, Averous L (2001) Polymer 42:6209
23. Carvalho AJF, Curvelo AAS, Gandini A (2005) Ind Crops Prod 21:331
24. Sheth M, Kumar RA, Davé V, Gross RA, McCarthy SP (1997) J Appl Polym Sci 66:1495
25. Nature Works LLC Reports (2011) http://www.natureworksllc.com. Accessed 5 January 2011
26. Luo WJ, Li SM, Bei JZ, Wang SG (2002) J Appl Polym Sci 84:1729
27. Nijenhuis AJ, Colstee E, Grijpma DW, Pennings AJ (1996) Polymer 37:5849
28. Pillin I, Montrelay N, Grohens Y (2006) Polymer 47:4676
29. Pereira AGB, Gollveia RF, de Carvalho GM, Rubira AF, Muniz EC (2009) Mater Sci Eng, C 29:499
30. Kim C-H, Kim D-W, Cho KY (2009) Polym Bull 63:91
31. Lourdin D, Bizot H, Colonna P (1997) J Appl Polym Sci 63:1047
32. Sarazin P, Li G, Orts WJ, Favis BD (2008) Polymer 49:599
33. Craig DQM (1995) Themochim Acta 248:189
34. Bogdanov B, Vidts A, Bulcke VD, Verbeeck R, Schacht E (1998) Polymer 39:1631
35. Read BE (1962) Polymer 3:529
36. Cassu SN, Felisberti MI (1997) Polymer 38:3907
37. Cartier L, Okihara T, Ikada Y, Tsuji H, Puiggali J, Lotz B (2000) Polymer 41:8909
38. Fischer EW, Sterzel HJ, Wegner G, Kolloid ZZ (1973) Polymer 25:980
39. Beaumont RH, Clegg B, Gee G, Herbert JBM, Marks DJ, Roberts RC, Sims D (1966) Polymer 7:401
40. Schlemmer D, de Oliveira ER, Sales MJA, Thermal J (2007) Anal Calorim 87:635
41. Yokesahachart C, Yoksan R (2011) Carbohydr Polym 83:22
42. Shi QF, Chen C, Gao L, Jiao L, Xu H, Guo W (2011) Polym Degrad Stab 96:175
43. McNeill IC, Leiper HA (1985) Polym Degrad Stab 11:309
44. Zeng QH, Yu AB, Lu GQ, Paul DR (2005) J Nanosci Nanotechnol 5:1574
45. Aggarwal P, Dollimore D, Heon K (1997) J Thermal Anal 50:7